Current Biology 24, 839–844, April 14, 2014 ©2014 Elsevier Ltd All rights reserved http://dx.doi.org/10.1016/j.cub.2014.02.060

Report

MUT-14 and SMUT-1 DEAD Box RNA Helicases Have Overlapping Roles in Germline RNAi and Endogenous siRNA Formation

Carolyn M. Phillips,[1,2] Brooke E. Montgomery,[3] Peter C. Breen,[1,2] Elke F. Roovers,[4] Young-Soo Rim,[1,2,6] Toshiro K. Ohsumi,[1,2,7] Martin A. Newman,[1,2] Josien C. van Wolfswinkel,[5,8] Rene F. Ketting,[4,5] Gary Ruvkun,[1,2,*] and Taiowa A. Montgomery[3,*]

[1]Department of Molecular Biology, Massachusetts General Hospital, Boston, MA 02114, USA
[2]Department of Genetics, Harvard Medical School, Boston, MA 02114, USA
[3]Department of Biology, Colorado State University, Fort Collins, CO 80523, USA
[4]Institute of Molecular Biology, 55128 Mainz, Germany
[5]Hubrecht Institute-KNAW and University Medical Centre Utrecht, 3584 CT Utrecht, the Netherlands

Summary

More than 2,000 *C. elegans* genes are targeted for RNA silencing by the *mutator* complex, a specialized small interfering RNA (siRNA) amplification module which is nucleated by the Q/N-rich protein MUT-16. The *mutator* complex localizes to *Mutator* foci adjacent to P granules at the nuclear periphery in germ cells [1]. Here, we show that the DEAD box RNA helicase *smut-1* functions redundantly in the *mutator* pathway with its paralog *mut-14* during RNAi. Mutations in both *smut-1* and *mut-14* also cause widespread loss of endogenous siRNAs. The targets of *mut-14* and *smut-1* largely overlap with the targets of other *mutator* class genes; however, the *mut-14 smut-1* double mutant and the *mut-16* mutant display the most dramatic depletion of siRNAs, suggesting that they act at a similarly early step in siRNA formation. *mut-14* and *smut-1* are predominantly expressed in the germline and, unlike other *mutator* class genes, are specifically required for RNAi targeting germline genes. A catalytically inactive, dominant-negative missense mutant of MUT-14 is RNAi defective in vivo; however, *mutator* complexes containing the mutant protein retain the ability to synthesize siRNAs in vitro. The results point to a role for *mut-14* and *smut-1* in initiating siRNA amplification in germ cell *Mutator* foci, possibly through the recruitment or retention of target mRNAs.

Results and Discussion

mut-14 and *smut-1* Have Overlapping Roles in Germline RNAi

22G siR-1 is one of a cluster of secondary 22 nt 5′G-containing small interfering RNAs (siRNAs) (22G-RNAs) produced from the long noncoding RNA *linc-22* [2]. 22G siR-1 formation requires each of the six *mutator* class genes except the DEAD box RNA helicase *mut-14* [1]. Consistent with their roles in 22G siR-1 formation, an siR-1 sensor transgene [3] is desilenced in each *mutator* mutant except *mut-14(pk738)* (Figure 1A). Each mutant assayed is presumed null, containing early stop codons or large deletions, except *mut-14(pk738)*, which encodes a protein bearing an amino acid substitution in the conserved catalytic core of the DEAD motif. To generate a null allele of *mut-14*, *mut-14(mg464)*, hereafter referred to simply as *mut-14*, we deleted the *mut-14* coding sequence [4]. Animals containing the *mut-14(pk738)* point mutation were deficient in their ability to inactivate germline mRNAs by RNAi but competent to inactivate somatic mRNAs by RNAi (Figure 1B) [1]. In contrast, animals containing the *mut-14* deletion were competent for both germline and somatic gene inactivations by RNAi, similar to the wild-type (Figure 1B).

Y38A10A.6, hereafter referred to as *synthetic* mut*ator-1* (*smut-1*), is one of two closely related paralogs of *mut-14*, although unlike MUT-14, *smut-1* contains a serine instead of an alanine within its DEAD motif (DESD) (Figures S1A and S1B available online). Similar to the *mut-14* deletion and to the wild-type, *smut-1(tm1301)*, a strain containing a large deletion in *smut-1*, was susceptible to both germline and somatic RNAi. In contrast, a strain carrying deletions in both *mut-14* and *smut-1* was defective for germline RNAi but normal for somatic RNAi, similar to *mut-14(pk738)* (Figure 1B). ZC317.1, the other closely related paralog of *mut-14* (Figure S1A), is predicted by RNA sequencing [5] to contain an early stop codon that truncates the C-terminal helicase domain (Figures S1B and S1C). We did not observe RNAi defects in a ZC317.1 deletion mutant, nor did we observe somatic RNAi defects in animals containing mutations in all three related helicases (Figure S1D).

GFP expression from the siR-1 sensor was strongly elevated in both the *mut-14(pk738) smut-1* and *mut-14 smut-1* double mutants, but not in *mut-14* or *smut-1* single-deletion mutants (Figures 1C, S1E, and S1F). 22G siR-1 levels were moderately reduced in *smut-1* ($p = 0.026$) and to a greater degree in the *mut-14 smut-1* double mutant ($p < 0.001$), but not in the *mut-14* single mutant (Figure S1G). The levels of each of two ERGO-1 class 26G-RNAs, which act upstream of the production of certain 22G-RNAs, were also significantly reduced in the *mut-14 smut-1* double mutant ($p < 0.05$), but not in either single mutant (Figure S1G). Although 22G siR-1 is somatic, its formation is initiated by an ERGO-1 class 26G-RNA during oogenesis and/or embryogenesis [3]; thus, it is possible that *mut-14* and *smut-1* are indirectly involved in 22G siR-1 formation in the soma via their role in 26G-RNA formation in the germline.

Consistent with a requirement for *mut-14* and *smut-1* specifically in germline RNAi, *mut-14* and *smut-1* promoters drive expression of mCherry predominantly in germ cells (Figure 1D). mCherry expression from the *smut-1* promoter, but not the *mut-14* promoter, was also relatively strong in developing embryos (Figure S1H).

Widespread Loss of Endogenous siRNAs in *mut-14 smut-1*

We sequenced small RNAs from the wild-type and from *mut-14* and *smut-1* single and double mutants, each of which

[6]Present address: Department of Developmental Biology, Stanford University School of Medicine, Stanford, CA 94305, USA
[7]Present address: Seres Health Inc., Cambridge, MA 02142, USA
[8]Present address: Whitehead Institute, Department of Biology, Massachusetts Institute of Technology, Cambridge, MA 02142, USA
*Correspondence: ruvkun@molbio.mgh.harvard.edu (G.R.), tai.montgomery@colostate.edu (T.A.M.)

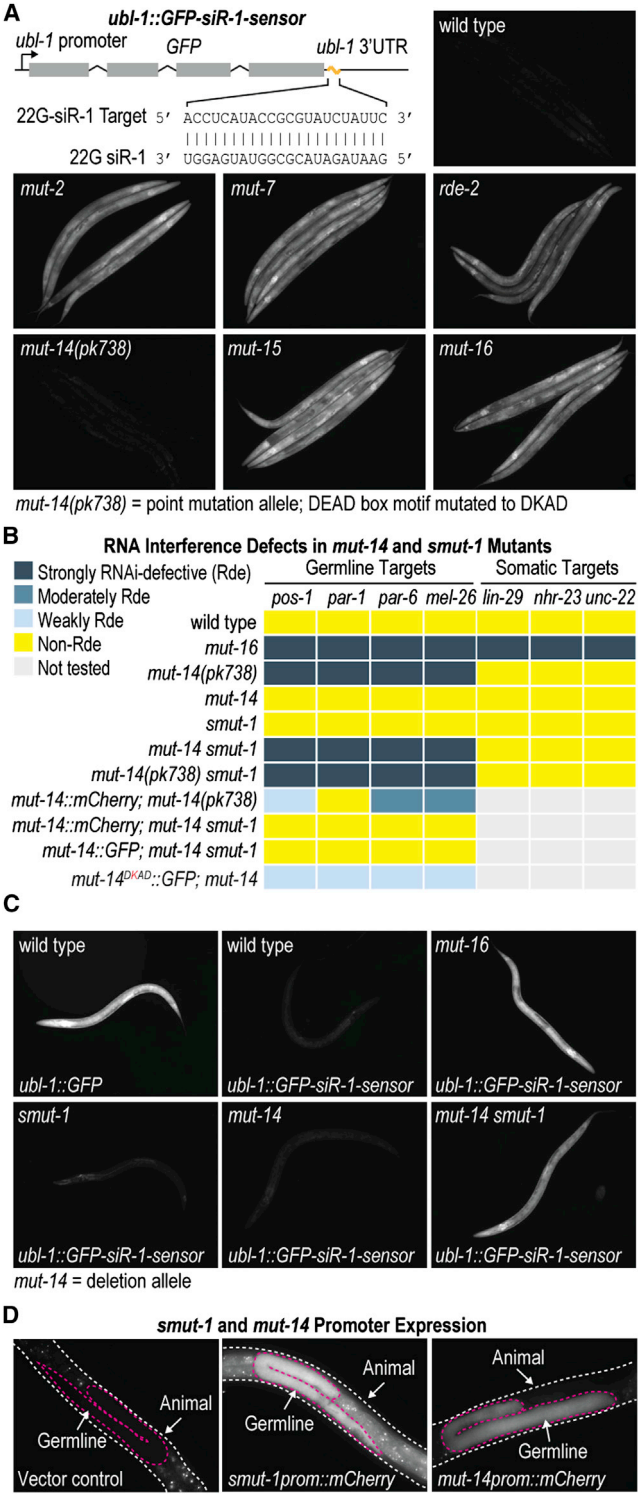

Figure 1. *mut-14* and *smut-1* Have Redundant Roles in RNAi

(A) Diagram of the 22G siR-1 sensor *ubl-1::GFP-siR-1-sensor* and images of GFP fluorescence from transgenic wild-type and mutant larval stage L4 animals.

(B) Assay for germline and somatic RNA interference defects.

(C) Images of L4 stage animals containing either the *ubl-1::GFP* control transgene, which lacks a 22G siR-1 target site, or the *ubl-1::GFP-siR-1-sensor* transgene.

(D) mCherry expression from *smut-1* and *mut-14* promoter fusions in L4 animals. Animals are outlined in white, and gonads are outlined in magenta. The vector control lacks *mCherry* sequence and is shown as a control for autofluorescence.

See also Figure S1.

also contained the siR-1 sensor transgene (Table S1). *smut-1* displayed very little change in siRNA levels across each of the six *C. elegans* chromosomes, relative to the wild-type, whereas *mut-14* displayed widespread but modest loss of siRNAs, which was strongly enhanced in the *mut-14 smut-1* double mutant (Figure 2A). siRNAs depleted in *mut-14* and *mut-14 smut-1* were predominantly 22G-RNAs derived from coding genes, pseudogenes, and transposons (Figure 2B). We identified 2,335 coding genes, pseudogenes, and transposons that were depleted of siRNAs by >3-fold in *mut-14 smut-1* (Figure 2C).

To determine which classes of siRNAs are dependent on *mut-14* and *smut-1*, we examined 22G-RNA levels from mRNA targets of the Argonautes WAGO-1, CSR-1, ERGO-1, and ALG-3/ALG-4, which represent each of the *C. elegans* endogenous siRNA pathways [6–10]. ERGO-1 and ALG-3/ALG-4 bind 26G-RNAs but trigger formation of 22G-RNAs from target mRNAs [6, 9, 11]. 22G-RNAs derived from WAGO and ERGO-1 targets were strongly depleted in the *mut-14 smut-1* double mutant but only modestly or not at all in the single mutants (Figure 2D). In contrast, the levels of 22G-RNAs derived from ALG-3/ALG-4 targets were not substantially affected in any of the *mut-14* and *smut-1* mutants, nor were the levels of primary ALG-3/ALG-4 class 26G-RNAs (Figures 2D and S1G). CSR-1 class siRNA levels appeared to be elevated in the *mut-14 smut-1* double mutant, possibly a normalization artifact caused by reduced levels of WAGO and ERGO-1 class siRNAs, as a CSR-1 siRNA that we examined by qRT-PCR was unaffected (Figures 2D and S1G).

The siR-1 sensor is subject to transgene silencing in the germline, independent of 22G siR-1 [3]. siRNAs derived from the siR-1 sensor were depleted in *mut-14* and to a greater extent in the *mut-14 smut-1* double, but not in the *smut-1* single, mutant (Figures 2D–2E). We conclude that *mut-14* and *smut-1* have overlapping roles in WAGO and ERGO-1 pathways, transgene silencing, and exogenous RNAi, although their roles in these pathways may be restricted to the germline and early embryos.

Catalytically Dead *mut-14*(*pk738*) Is Antagonistic to *smut-1*

mut-14(pk738) encodes a protein bearing a point mutation that alters an amino acid in the DEAD motif and, unlike the *mut-14* deletion allele, is germline RNAi defective (Figure 1B). We sequenced small RNAs from the wild-type and from *mut-14(pk738)* and *smut-1* single and double mutants (Table S1). The proportion of features depleted of siRNAs was similar between *mut-14(pk738)* and the *mut-14(pk738) smut-1* double mutant (Figure 2F). The vast majority of genes depleted of siRNAs in the *mut-14(pk738) smut-1* double mutant were also affected in the *mut-14(pk738)* single mutant (Figure 2G). WAGO class 22G-RNAs were depleted to similar levels in *mut-14(pk738)* and the *mut-14(pk738) smut-1* double mutant (Figure 2H), both of which resemble the depletion seen in the *mut-14 smut-1* double deletion mutant (Figure 2D). In contrast, 22G-RNA levels from ERGO-1 targets were somewhat elevated in *mut-14(pk738)* but depleted by ~80% in *mut-14(pk738) smut-1*, similar to what was observed in the *mut-14 smut-1* deletion mutant (Figures 2D and 2H). When fused to mCherry or GFP, wild-type MUT-14 and MUT-14

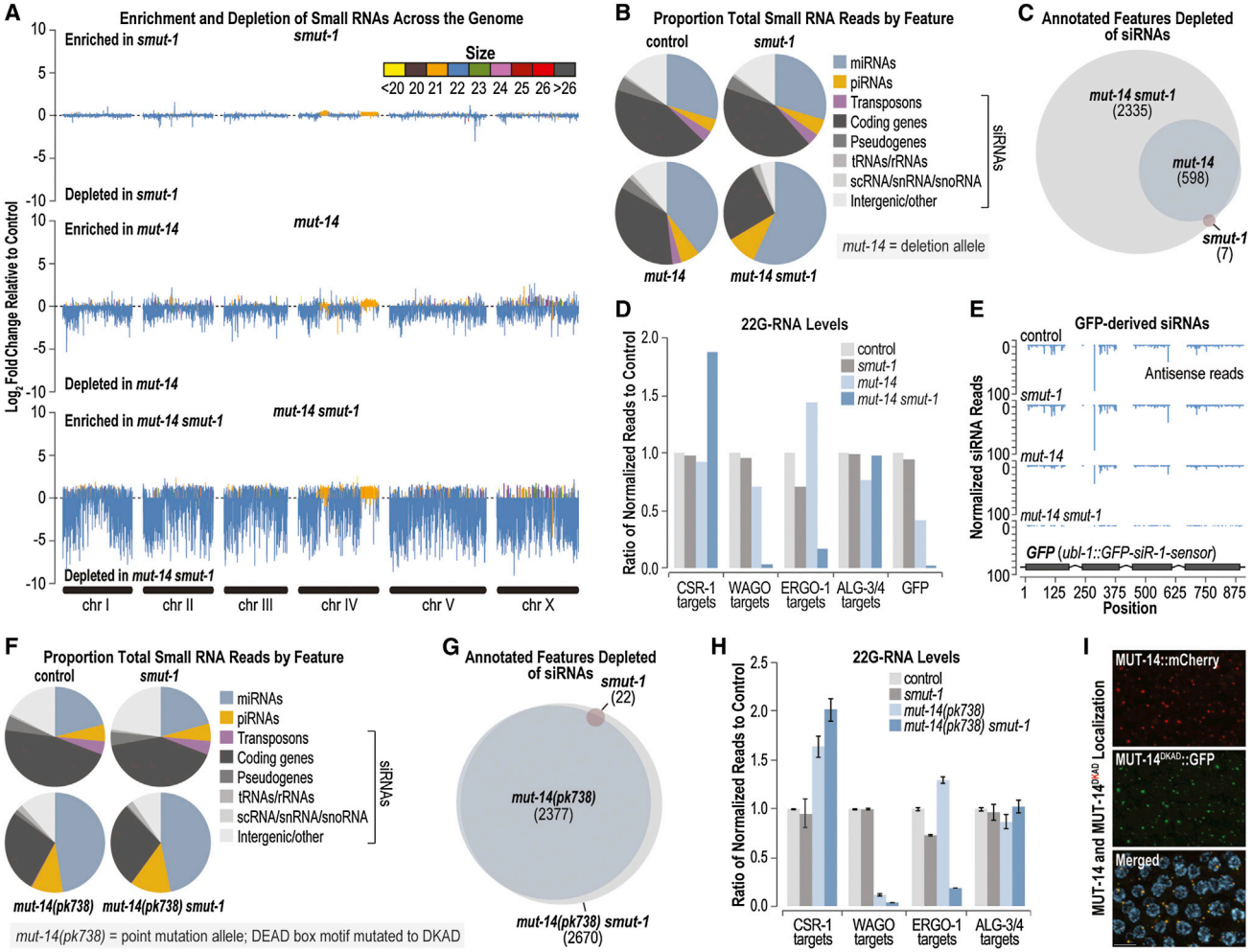

Figure 2. *mut-14 smut-1* Mutants Display Widespread Loss of Endogenous siRNAs

(A) Log_2 ratio of small RNA reads in *smut-1*, *mut-14*, and *mut-14 smut-1* mutants, relative to control animals, plotted across each chromosome. Each strain also contains the *ubl-1::GFP-siR-1-sensor* transgene. Control animals contain the siR-1 sensor but are wild-type for *smut-1* and *mut-14*. Peaks are colored based on the dominant size class.

(B) Proportion of small RNA reads aligning to each genomic feature.

(C) The Venn diagram displays genes depleted of siRNAs in *smut-1* and *mut-14* mutants. Total numbers of targets depleted of siRNAs by >3-fold in each mutant, relative to the wild-type, are indicated in parentheses.

(D) Relative levels of 22G-RNAs in *smut-1* and *mut-14* mutants (sequencing was done without replicates).

(E) Normalized GFP siRNA reads from the *ubl-1::GFP-siR-1-sensor* transgene. For simplicity, the 22G siR-1 target site and downstream sequence is not shown.

(F) Proportion of small RNA reads aligning to each genomic feature.

(G) The Venn diagram displays genes depleted of siRNAs in *smut-1* and *mut-14(pk738)* mutants. Total numbers of targets depleted of siRNAs by > 3-fold in each mutant, relative to wild-type, are indicated in parentheses.

(H) Relative levels of 22G-RNAs in *smut-1* and *mut-14(pk738)* mutants. Mean ± SD for two biological replicates.

(I) MUT-14::mCherry (red) and catalytically dead MUT-14^{DKAD}::GFP (green) colocalization at perinuclear *Mutator* foci. DNA is counterstained with DAPI (blue).

See also Figure S1 and Table S1.

containing the *pk738* mutation (MUT-14^{DKAD}) colocalized at the nuclear periphery, indicating that *mut-14(pk738)* produces a stable protein that localizes to the proper compartment (Figure 2I).

These results suggest that *mut-14*(*pk738*) is antagonistic to *smut-1* during WAGO class 22G-RNA formation. That *mut-14*(*pk738*) is not antagonistic to *smut-1* in ERGO-1 class 26G-RNA and *ergo-1*-dependent 22G-RNA formation may be related to differential expression of *smut-1* and *mut-14* during oogenesis and embryogenesis, the stages during which 26G-RNAs are produced (Figure S1H) [6, 10].

Comprehensive Analysis of siRNA Defects in *Mutator* Mutants

MUT-14 is part of an siRNA amplification module that includes the *mutators* MUT-2, MUT-7, RDE-2, MUT-15, and MUT-16 and which colocalizes with the RNA-dependent RNA polymerase RRF-1 [1]. To determine whether *mut-14*, *smut-1*, and the other *mutators* converge on a common set of targets, we subjected wild-type and mutant animals to small RNA sequencing (Table S1). Each of the *mutator* mutants was depleted of 22G-RNAs derived from WAGO and ERGO-1 targets, but not substantially from CSR-1 or ALG-3/ALG-4 targets (Figure 3A).

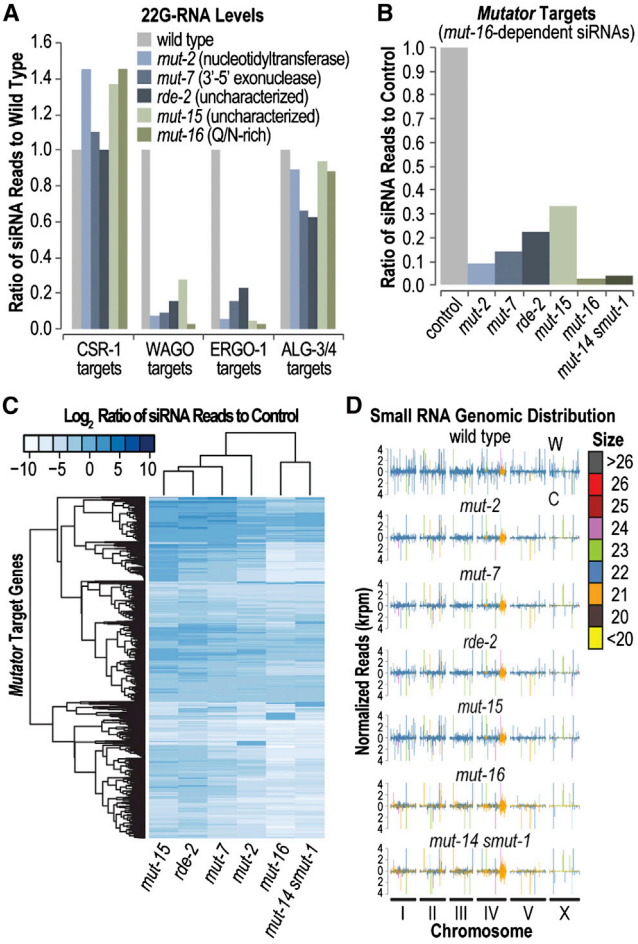

Figure 3. *mut-14 smut-1* and *mut-16* Mutants Have Similar siRNA Defects

(A) Relative levels of 22G-RNAs in the wild-type and *mut-2*, *mut-7*, *rde-2*, *mut-15*, and *mut-16* mutants.

(B) Relative levels of 22G-RNAs derived from *mutator* target mRNAs in each of the *mutator* mutants, relative to the wild-type or a similar control.

(C) The heatmap displays the $\log_2$ ratio of siRNA reads in each mutant, relative to the wild-type or a similar control, for each of the *mutator* target genes.

(D) Normalized small RNA reads (thousand reads per million total library reads) in the wild-type and each of the *mutator* mutants plotted across each chromosome. Peaks are colored based on the dominant size class. siRNAs are predominantly 22 nt in wild-type animals. W, Watson strand; C, Crick strand.

See also Figure S2 and Tables S1 and S2.

Although the genes depleted of siRNAs in each of the *mutator* mutants largely overlapped, *mut-16* displayed the greatest loss of siRNAs (Figures 3A and S2A). Thus, we defined *mutator* targets as the ~2,300 genes depleted of siRNAs by >3-fold in *mut-16* (Table S2). Of the six *mutator* mutants, *mut-16* and the *mut-14 smut-1* double mutant showed the strongest depletion of siRNAs from *mutator* targets (Figure 3B and Table S2). When clustered by depletion in *mutator* target siRNAs, *mut-16* and the *mut-14 smut-1* double mutant assembled more closely with one another than with any of the other *mutator* mutants (Figure 3C).

There was a genome-wide enrichment, particularly from *mutator* target genes, for 21 nt small RNA species in *mut-16* and *mut-14 smut-1* mutants, but not in any of the other *mutator* mutants (Figures 3D and S2B–S2D). We examined residual siRNAs in each *mutator* mutant to determine whether they contained modifications that were absent in wild-type animals that might to point to a specific role in siRNA maturation. We observed an ~3-fold increase in the proportions of siRNAs containing nontemplated 3′ uracil (U) additions in *mut-16* and *mut-14 smut-1* but not in any of the other *mutator* mutants (Figure S2E). The proportion of siRNAs containing 3′ nontemplated Us was elevated ~8.5-fold in the *mut-14*(*pk738*) *smut-1* double mutant, and nearly every siRNA-yielding gene had elevated levels of nontemplated Us, including CSR-1 targets (Figures S2E–S2F). The reason for this is unclear; however, the size distribution and elevated levels of nontemplated Us observed in residual siRNAs in *mut-16* and *mut-14 smut-1* are features more common to CSR-1 class siRNAs than to WAGO class (Figure S2G) [3, 8, 12]. It is possible that some *mutator* targets also produce CSR-1 class siRNAs or that in the absence of the *mutator* pathway some *mutator* targets are misrouted into the CSR-1 pathway.

We did not find evidence for siRNA precursors in any of our libraries, although our analysis was limited to sequences <30 nt long, which may indicate that the *mutators* function to facilitate RNA-dependent RNA polymerase activity on target mRNAs and are not involved in processing siRNAs into their 22 nt mature form. *mut-16*, but not *mut-14* or *smut-1*, is required for formation and proper localization of the *mutator* complex (Figure S2H) [1], indicating that *mut-16* acts upstream of other *mutators* during siRNA biogenesis. Because *mut-16* and the *mut-14 smut-1* double mutant have the most dramatic effects on siRNA levels and show similar anomalies in residual siRNAs, we propose that they act at a similarly early step in siRNA formation. Although *mut-14* and *smut-1* are not required for *mutator* protein localization, they could be required to recruit mRNAs into *Mutator* foci to initiate siRNA amplification.

Compartmentalization of the *Mutator* Pathway Is Restricted to the Germline

Each of the *mutators* except *mut-14* and *smut-1* are required for both somatic and germline RNAi [1]. It is possible that another gene fulfills the function in somatic cells that *mut-14* and *smut-1* serve in the germline. Alternatively, *mut-14* and *smut-1* could have a role in RNAi that is specifically required in germ cells. What distinguishes germline RNAi from somatic RNAi? In germ cells, each of the *mutator* proteins localize to perinuclear compartments, called *Mutator* foci, adjacent to P granules [1]. To determine whether the *mutators* are also compartmentalized in the soma, we examined GFP expression in animals containing either the *mut-16* promoter (*mut-16prom::GFP*) or the *mut-16* promoter and coding sequence fused to GFP (*mut-16::GFP*). *mut-16* is required for *mutator* complex formation in both the soma and the germline and for its localization to the nuclear periphery in germ cells [1]. Free GFP expressed from the *mut-16* promoter was present throughout the germline and soma, in contrast to *mut-14* and *smut-1*, which are predominantly expressed in the germline (Figures 1D and 4A). The MUT-16::GFP translational fusion protein formed distinct perinuclear foci in the germline but appeared to be diffuse throughout the cytoplasm in somatic cells (Figures 4A and S3A). MUT-7::GFP also appeared to be diffuse in somatic cells, indicating that the *mutators* are not compartmentalized in the soma, consistent with our previous observations (Figure S3B) [1]. Thus, there are at least two features that distinguish germline RNAi from somatic RNAi: (1) the requirement

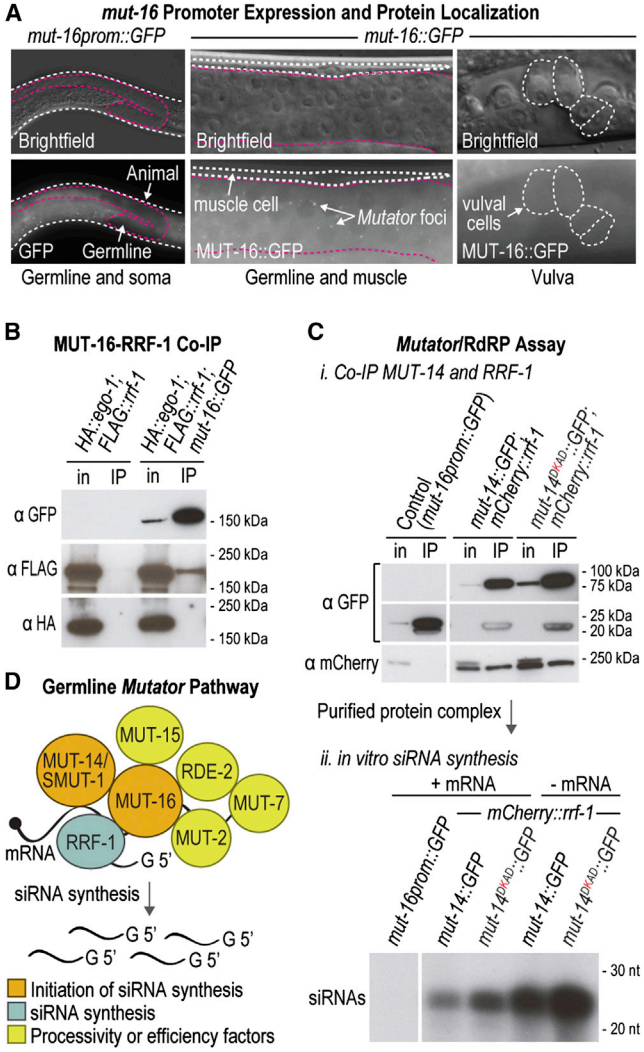

Figure 4. *Mutator* Complex Containing Catalytically Dead MUT-14 Is Competent for siRNA Formation In Vitro

(A) Expression and localization of GFP derived from a *mut-16* transcriptional fusion (*mut-16prom::GFP*) and a *mut-16* translational fusion (*mut-16::GFP*) in adult animals. *Mutator* foci and muscle and vulval cells are indicated.

(B) Western blot analysis of MUT-16::GFP, FLAG::RRF-1, and HA::EGO-1 from cell lysates (in) and anti-GFP coimmunoprecipitates (IP).

(C) Top: in vitro assay for siRNA synthesis. Western blot analysis of free GFP (*mut-16prom::GFP*) and GFP and mCherry fusion proteins (*mut-14::GFP*; *mCherry::rrf-1; mut-14 smut-1* and *mut-14^{DKAD}::GFP; mCherry::rrf-1; mut-14*) from cell lysates (in) and anti-GFP coimmunoprecipitates (IP). A faint background band is observed in each of the input samples after probing with mCherry antibody. Bottom: In vitro synthesized siRNAs following coimmunoprecipitation of *mutator* complexes containing wild-type MUT-14 (*mut-14::GFP; mCherry::rrf-1; mut-14 smut-1*) or catalytically dead MUT-14 (*mut-14^{DKAD}::GFP; mCherry::rrf-1; mut-14*). Immunoprecipitated protein complexes were incubated with a mixture of radiolabeled and nonlabeled nucleotides and in the presence or absence of an in vitro-transcribed mRNA (B0250.8).

(D) Schematic depicting siRNA formation by the *mutator* complex in the germline.

See also Figure S3 and Tables S3 and S4.

for either *mut-14* or *smut-1* and (2) compartmentalization of the *mutator* complex. Therefore, it is possible that the role of *mut-14* and *smut-1* is related to compartmentalization of the RNAi pathway.

MUT-14 Catalytic Activity Is Dispensable for siRNA Formation In Vitro

We performed a yeast two-hybrid screen to test *mutator* protein interactions with other validated and predicted small RNA factors, including SMUT-1, which was identified in a screen for gene inactivations that desilence an RNAi sensor (Table S3) [13, 14]. As predicted by its role in nucleating the *mutator* complex and its prion-like Q/N-rich region, MUT-16 was the most promiscuous factor, binding to 12 of the 58 proteins assayed. MUT-16 interactors included the *mutators* SMUT-1 and RDE-2, the Argonautes WAGO-1 and ERGO-1, the RNA-dependent RNA polymerase EGO-1, and several chromatin factors, including MES-4 and GFL-1 (Figure S3C and Table S4). These results are consistent with the requirement for *mut-16* in siRNA formation from WAGO and ERGO-1 targets and point to a direct interaction between MUT-16 and SMUT-1. EGO-1 may not associate with MUT-16 in vivo in wild-type animals, as we did not observe EGO-1 at *Mutator* foci [1]. Furthermore, in MUT-16::GFP immunoprecipitates we detected FLAG::RRF-1, but not HA::EGO-1 (Figure 4B). *ego-1* functions redundantly with *rrf-1* [7], suggesting that in the absence of *rrf-1*, EGO-1 might bind to MUT-16. In coimmunoprecipitation assays of mCherry::EGO-1 and MUT-16::GFP, we detected only a very weak interaction between EGO-1 and MUT-16 in *rrf-1* mutants (Figure S3D). EGO-1 also functions in the CSR-1 pathway in P granules and therefore may have a stronger affinity for factors involved in CSR-1 class siRNA formation than for the *mutators* [7, 8].

Because RRF-1 coimmunoprecipitates with MUT-16 and is therefore associated with the *mutator* complex, we reasoned that we could pull down any factor in the complex and perform siRNA synthesis in vitro. This would allow us to test whether or not complexes containing wild-type or catalytically dead MUT-14 are competent for siRNA synthesis in an in vitro context in which the pathway is not compartmentalized. We immunoprecipitated wild-type MUT-14 (MUT-14::GFP) and catalytically dead MUT-14 (MUT-14^{DKAD}::GFP) and incubated the purified complexes with a mixture of radiolabeled and nonlabeled ribonucleotides. Both MUT-14::GFP and MUT-14^{DKAD}::GFP coimmunoprecipitated mCherry::RRF-1 (Figure 4C). Complexes containing either wild-type or catalytically dead MUT-14 immunoprecipitated from *mut-14* or the *mut-14 smut-1* double mutant were proficient for siRNA synthesis (Figures 4C and S3E). In contrast, a control immunoprecipitate containing free GFP (*mut-16prom::GFP*) failed to produce siRNAs, as did FLAG::RRF-1 complex immunoprecipitated from *mut-16* mutants in which the *mutator* complex does not form (Figures 4C and S3E) [1]. Addition of an in vitro-transcribed B0250.8 mRNA, an endogenous target of *mut-14* and *smut-1* (Table S2), was not necessary and was actually inhibitory to siRNA formation, indicating that the complex coimmunoprecipitated RNA (Figure 4C). It is unclear whether the complex contained RNA in vivo or whether it bound RNA during incubation of the cell lysate with GFP antibody.

Our results demonstrate that *mut-14* and *smut-1* are not required for RNAi in the soma or for siRNA formation in vitro, two distinct contexts in which the *mutator* complex is not compartmentalized. Nor are they required for localization of other *mutator* proteins. Yet the data point to an essential role for *mut-14* and *smut-1* at an early step in siRNA formation in the germline, in which the *mutator* complex is compartmentalized. DEAD box helicases have numerous roles in RNA processing, such as localized unwinding of RNA duplexes and as RNA

clamps [15]. Vasa, which is closely related to MUT-14 and SMUT-1 (blastp p values $\leq 5 \times 10^{-19}$, 24% identity), functions along with UAP56 in the *Drosophila* germline to transport RNA from the site of transcription in the nucleus to perinuclear piRNA processing compartments called nuage [16]. It is possible that MUT-14 and SMUT-1 are involved in transporting mRNAs from P granules, sites of mRNA surveillance, into *Mutator* foci nucleated by MUT-16 to initiate siRNA amplification. The more modest reduction in siRNA levels in the other *mutators* suggests that they serve accessory roles in siRNA biogenesis (Figure 4D).

Experimental Procedures

mut-14(mg464) and ZC317.1*(mgDf465)* deletion alleles were generated using MosDEL [4]. Transgenes were generated using Life Technologies Multisite Gateway Technology and introduced into *C. elegans* using MosSCI (Table S5) [17]. *C. elegans* were cultured at 20°C [18]. Immunofluorescence assays were done as described [1]. For yeast two-hybrid assays, candidate gene sequences were cloned into bait and prey vectors using Gateway Technology and then transformed into *Saccharomyces cerevisiae GAL4* and *GAL80* deletion strains Y8800 (prey, MATa) and Y8930 (bait, MATα). For assessment of RNAi defects in *mutator* mutants, animals were fed *E. coli* expressing double-stranded RNA with sequence homology to germline or somatic genes. Taqman quantitative RT-PCR assays were done as described (Table S5) [10]. Small RNA sequencing was done as described [3]. Sequences were aligned to the *C. elegans* reference genome WS204 using CASHX v. 2.0 [19]. Coimmunoprecipitation and western blot assays were done as described [1]. RdRP assays were done as described [20].

Accession Numbers

The NCBI Gene Expression Omnibus accession number for the small RNA high-throughput sequencing data reported in this paper is GSE54320.

Supplemental Information

Supplemental Information includes Supplemental Experimental Procedures, three figures, and five tables and can be found with this article online at http://dx.doi.org/10.1016/j.cub.2014.02.060.

Acknowledgments

Thanks to Ulandt Kim and Yanqun Wang for Illumina sequencing. Strains were provided by the Caenorhabditis Genetics Center, which is funded by the NIH Office of Research Infrastructure Programs (P40 OD010440), and Shohei Mitani of the Japanese National Bioresources Project. Mos strains were generated by the Ewbank and Segalat labs as part of the NEMAGENETAG project funded by the European Community and distributed by M. Carre-Pierrat at the UMS 3421, supported by the CNRS. This work was supported by the NIH (GM44619 to G.R.), Colorado State University (T.A.M.), the Massachusetts General Hospital Executive Committee of Research (C.M.P. and T.A.M.), the Damon Runyon Cancer Research Foundation (C.M.P. and T.A.M.), and an ERC Starting Grant (202819) from the Ideas Program of the European Union Seventh Framework Program (R.F.K.).

Received: November 19, 2013
Revised: February 4, 2014
Accepted: February 28, 2014
Published: March 27, 2014

References

1. Phillips, C.M., Montgomery, T.A., Breen, P.C., and Ruvkun, G. (2012). MUT-16 promotes formation of perinuclear mutator foci required for RNA silencing in the C. elegans germline. Genes Dev. *26*, 1433–1444.
2. Nam, J.-W., and Bartel, D.P. (2012). Long noncoding RNAs in C. elegans. Genome Res. *22*, 2529–2540.
3. Montgomery, T.A., Rim, Y.-S., Zhang, C., Dowen, R.H., Phillips, C.M., Fischer, S.E.J., and Ruvkun, G. (2012). PIWI associated siRNAs and piRNAs specifically require the Caenorhabditis elegans HEN1 ortholog henn-1. PLoS Genet. *8*, e1002616.
4. Frøkjaer-Jensen, C., Davis, M.W., Hollopeter, G., Taylor, J., Harris, T.W., Nix, P., Lofgren, R., Prestgard-Duke, M., Bastiani, M., Moerman, D.G., and Jorgensen, E.M. (2010). Targeted gene deletions in C. elegans using transposon excision. Nat. Methods *7*, 451–453.
5. Gerstein, M.B., Lu, Z.J., Van Nostrand, E.L., Cheng, C., Arshinoff, B.I., Liu, T., Yip, K.Y., Robilotto, R., Rechtsteiner, A., Ikegami, K., et al.; modENCODE Consortium (2010). Integrative analysis of the Caenorhabditis elegans genome by the modENCODE project. Science *330*, 1775–1787.
6. Vasale, J.J., Gu, W., Thivierge, C., Batista, P.J., Claycomb, J.M., Youngman, E.M., Duchaine, T.F., Mello, C.C., and Conte, D., Jr. (2010). Sequential rounds of RNA-dependent RNA transcription drive endogenous small-RNA biogenesis in the ERGO-1/Argonaute pathway. Proc. Natl. Acad. Sci. USA *107*, 3582–3587.
7. Gu, W., Shirayama, M., Conte, D., Jr., Vasale, J., Batista, P.J., Claycomb, J.M., Moresco, J.J., Youngman, E.M., Keys, J., Stoltz, M.J., et al. (2009). Distinct argonaute-mediated 22G-RNA pathways direct genome surveillance in the C. elegans germline. Mol. Cell *36*, 231–244.
8. Claycomb, J.M., Batista, P.J., Pang, K.M., Gu, W., Vasale, J.J., van Wolfswinkel, J.C., Chaves, D.A., Shirayama, M., Mitani, S., Ketting, R.F., et al. (2009). The Argonaute CSR-1 and its 22G-RNA cofactors are required for holocentric chromosome segregation. Cell *139*, 123–134.
9. Conine, C.C., Batista, P.J., Gu, W., Claycomb, J.M., Chaves, D.A., Shirayama, M., and Mello, C.C. (2010). Argonautes ALG-3 and ALG-4 are required for spermatogenesis-specific 26G-RNAs and thermotolerant sperm in Caenorhabditis elegans. Proc. Natl. Acad. Sci. USA *107*, 3588–3593.
10. Han, T., Manoharan, A.P., Harkins, T.T., Bouffard, P., Fitzpatrick, C., Chu, D.S., Thierry-Mieg, D., Thierry-Mieg, J., and Kim, J.K. (2009). 26G endo-siRNAs regulate spermatogenic and zygotic gene expression in Caenorhabditis elegans. Proc. Natl. Acad. Sci. USA *106*, 18674–18679.
11. Gent, J.I., Lamm, A.T., Pavelec, D.M., Maniar, J.M., Parameswaran, P., Tao, L., Kennedy, S., and Fire, A.Z. (2010). Distinct phases of siRNA synthesis in an endogenous RNAi pathway in C. elegans soma. Mol. Cell *37*, 679–689.
12. van Wolfswinkel, J.C., Claycomb, J.M., Batista, P.J., Mello, C.C., Berezikov, E., and Ketting, R.F. (2009). CDE-1 affects chromosome segregation through uridylation of CSR-1-bound siRNAs. Cell *139*, 135–148.
13. Kim, J.K., Gabel, H.W., Kamath, R.S., Tewari, M., Pasquinelli, A.E., Rual, J.-F., Kennedy, S., Dybbs, M., Bertin, N., Kaplan, J.M., et al. (2005). Functional genomic analysis of RNA interference in C. elegans. Science *308*, 1164–1167.
14. Robert, V.J., Sijen, T., van Wolfswinkel, J., and Plasterk, R.H.A. (2005). Chromatin and RNAi factors protect the C. elegans germline against repetitive sequences. Genes Dev. *19*, 782–787.
15. Linder, P., and Jankowsky, E. (2011). From unwinding to clamping - the DEAD box RNA helicase family. Nat. Rev. Mol. Cell Biol. *12*, 505–516.
16. Zhang, F., Wang, J., Xu, J., Zhang, Z., Koppetsch, B.S., Schultz, N., Vreven, T., Meignin, C., Davis, I., Zamore, P.D., et al. (2012). UAP56 couples piRNA clusters to the perinuclear transposon silencing machinery. Cell *151*, 871–884.
17. Frøkjaer-Jensen, C., Davis, M.W., Hopkins, C.E., Newman, B.J., Thummel, J.M., Olesen, S.-P., Grunnet, M., and Jorgensen, E.M. (2008). Single-copy insertion of transgenes in Caenorhabditis elegans. Nat. Genet. *40*, 1375–1383.
18. Brenner, S. (1974). The genetics of Caenorhabditis elegans. Genetics *77*, 71–94.
19. Fahlgren, N., Sullivan, C.M., Kasschau, K.D., Chapman, E.J., Cumbie, J.S., Montgomery, T.A., Gilbert, S.D., Dasenko, M., Backman, T.W.H., Givan, S.A., and Carrington, J.C. (2009). Computational and analytical framework for small RNA profiling by high-throughput sequencing. RNA *15*, 992–1002.
20. Tang, G., Reinhart, B.J., Bartel, D.P., and Zamore, P.D. (2003). A biochemical framework for RNA silencing in plants. Genes Dev. *17*, 49–63.